ACI STRUCTURAL JOURNAL TECHNICAL PAPER

Title no. 104-S50

Stress Analysis of Concrete Structures Subjected to Alkali-Aggregate Reactions

by Victor Saouma, Luigi Perotti, and Takashi Shimpo

In a separate paper, the authors have presented a constitutive model for the alkali-aggregate reaction (AAR) in concrete. This follow-up paper first examines how this complex and coupled model can be used for the long-term (until reaction exhaustion) prediction of an AAR-affected concrete structure. Then, through a series of parametric studies, sensitivity analyses are performed, and then basic modeling questions are addressed. Finally, the effect of AAR on the structural behavior of two dams and a reinforced concrete structure is presented.

Keywords: alkali-aggregate reaction; dams; stress.

INTRODUCTION

Many old concrete structures are known to suffer from alkali-aggregate reactions (AAR). This internal reaction causes gel formation inside the aggregate and the matrix and results in swelling of the concrete. This swelling in turn may cause secondary compressive stresses (if the structure is restrained, as most are), localized map cracks, and, ultimately structural cracks. In addition, the concrete tensile strength and elastic modulus can significantly decrease. One or a combination of these effects can cause major concern for massive concrete (such as dams) and for reinforced concrete structures. Indeed, as shown by Hatch Acres Corp. (2006), numerous dams worldwide are known to suffer from this reaction, for which there are no known effective remedies. Sealing the upstream face will only slow the swelling (though only marginally), and cutting the dam to relieve the stress build-up is only addressing the symptoms of the problem and not its causes. Indeed this is a major problem, and ideally the structural analysis should be able to predict the maximum expansion and accompanying deformation and damage.

Numerous dams worldwide are known to suffer from AAR (Hatch ACRES Corp. 2006). The Tennessee Valley Authority (TVA) has three major projects experiencing AAR, including the Fontana Dam and Powerhouse, Hiwassee Dam and Powerhouse, and Chickamauga Lock, Dam, and Powerhouse (Wagner and Newell 1995). All of these dams are more than 60 years old and are experiencing problems in one or more locations due to AAR, with no indication of any slowing of the concrete swelling. Some of the cracks were 0.5 in. (12 mm) wide by 1980. Other reports of the incidence of AAR on dams have been reported by Murtaugh (1995) concerning a dam intake tower; Gilks and Curtis (2003) for the Mactaquac Dam in Canada; Sinclair and Wark (2003) for the Canning Dam; Jabarooti and Golabtoonchi (2003) for an the Iranian dam; ICOLD (2001) for the Pian Telessio dam in Italy; the Portugese National Committee on Large Dams (2003) for the Pracana Dam; and Malla and Wieland (1999) for an arch gravity dam in Switzerland.

The effect of AAR on reinforced concrete beams (or cylinders) has been investigated by numerous researchers (Jones and Clark 1996; Ahmed et al. 1998; Monette et al. 2002; Fan and Hanson 1998; Mohammed et al. 2003; Multon et al. 2005). What seems to emerge from all these studies is that there is always a sigmoidal expansion. Hence, the reaction starts at a low rate, accelerates, and then slowly approaches an asymptotic value. In all cases, reinforcement inhibits expansion along its axis, and thus will essentially prestress the structure. This will result in possible upward camber and increased shear strength. Cracks will tend to align themselves with the longitudinal reinforcement and then the shear reinforcement (if present). Finally, the failure load does not seem to be affected by the AAR.

Saouma and Perotti (2006) have recently developed a comprehensive constitutive model for AAR in concrete. This coupled chemo-thermo-mechanical formulation was largely inspired by the extensive experimental research undertaken at the Laboratoire Central des Ponts et Chaussés by Larive (1998) and Multon et al. (2005). Though the model was thoroughly tested at the constitutive level for simple geometries, no detailed structural analysis has been reported. A more exhaustive and detailed literature survey can be found in Saouma and Perotti (2005).

With regard to structural analysis of AAR-affected structures, one must differentiate between the state of the art and the state of the practice. With regard to the former, there are many contenders, most of them relatively sophisticated models developed and used in the context of academic research (Huang and Pietruszczak 1999; Ulm et al. 2000; Li and Coussy 2002; Gomes et al. 2004; Bangert et al. 2004). All of these models have a kinetics model to account for the time dependency of the reaction, and most of them are based on a tight coupling between the chemical, thermal, hygral, and mechanical components.

On the other hand, and to the best of the authors' knowledge, the state-of-the-practice (Nuss 2005) appears to be based on an early (actually, one of the first) AAR model proposed by Charlwood et al. (1992) and Thompson et al. (1994). Computer programs based on these early models have been extensively used for major dam investigations. This early model accounted for the reduction of AAR expansion under compressive stresses, and had no kinetics component.

This paper will: 1) briefly review the pertinent literature and summarize key ingredients of the model; 2) describe the methodology adopted for the analysis and system identification of important AAR parameters; 3) present results of an extensive parametric study that assessed the relative importance of

ACI Structural Journal, V. 104, No. 5, September-October 2007.
MS No. S-2006-043.R4 received November 18, 2006, and reviewed under Institute publication policies. Pertinent discussion including author's closure, if any, will be published in the July-August 2008 *ACI Structural Journal* if the discussion is received by March 1, 2008.

ACI member **Victor Saouma** *is a Professor of civil engineering at the University of Colorado, Boulder, Colo., and Director of the NEES-NSF Fast Hybrid Testing NEES Laboratory. He is a member of ACI Committee 446, Fracture Mechanics, and Joint ACI-ASCE Committee 447, Finite Element Analysis of Reinforced Concrete Structures. His research interests are in dam engineering, earthquake engineering, concrete deterioration modeling, and fracture mechanics.*

Luigi Perotti *is a PhD Candidate at the California Institute of Technology. He graduated from the Department of Structural Engineering of the Technical Institute of Milan. His research interests include alkali-aggregate reactions (AAR).*

Takashi Shimpo *is an Engineer at the Research and Development Center of the Tokyo Electric Power Co., Yokohama, Japan. His research interests include AAR in reinforced concrete, heat island analysis, and dam engineering.*

various parameters; and 4) present three case studies investigated with the model.

RESEARCH SIGNIFICANCE

Despite the extensive literature on AAR, very few publications address the analysis of existing structures affected by AAR. This work presents a rigorous methodology to investigate massive and reinforced concrete structures affected by AAR, and then applies it to the actual analysis of three existing structures. Hence, the work bridges the gap between fundamental academic research and development and engineering practice.

Constitutive model

The theoretical underpinning of the model used in this paper has been separately presented by Saouma and Perotti (2006). It will be briefly reviewed. The AAR expansion is considered to be a volumetric one, whose rate is given by the following function

$$\dot{\varepsilon}_V^{AAR}(t) = \Gamma_t(f_t'|w_c, \sigma_I|COD_{max})\Gamma_c(\bar{\sigma}, f_c')g(H)\dot{\xi}(t,\theta)\varepsilon^{\infty}\big|_{\theta=\theta_0}$$

$$\Gamma_t = \begin{cases} 1 & \text{if } \sigma_I \le \gamma_t f_t' \\ \Gamma_r + (1-\Gamma_r)\dfrac{\gamma_t f_t^{fictitious}}{\sigma_I} & \text{if } \gamma_t f_t' < \sigma_I \end{cases};$$

$$\Gamma_c = \begin{cases} 1 & \text{if } \bar{\sigma} \le 0 \text{ Tension} \\ 1 - \dfrac{e^{\beta}\bar{\sigma}}{1+(e^{\beta}-1)\bar{\sigma}} & \text{if } \bar{\sigma} > 0 \text{ Compression} \end{cases}$$

$$\bar{\sigma} = \frac{\sigma_I + \sigma_{II} + \sigma_{III}}{3f_c'}; \quad g(H) = H^m$$

where $\varepsilon^{\infty}\big|_{\theta=\theta_0}$ is the final volumetric expansion as determined from laboratory tests at temperature θ_0. The expression $0 \le \Gamma_t \le 1$ is a function that reduces the expansion in the presence of large tensile stresses (macrocracks absorbing the gel). If an elastic model is used, then f_t' is the tensile strength and σ_I is the major (tensile) principal stress; H is the humidity. On the other hand, if a smeared crack model is adopted, then COD_{max} is the maximum crack opening displacement at the current Gauss point, and w_c is the maximum crack opening displacement in the tensile softening curve (Wittmann et al. 1988).

Similarly, $0 \le \Gamma_c \le 1$ is a function that accounts for the reduction in AAR volumetric expansion under relatively high compressive stresses (microcracks under compression and gel expansion reduction due to pluri-axial state of compressive stresses), and $\bar{\sigma}$ and f_t' are the hydrostatic stress and the compressive strength of the concrete, respectively. $0 \le g(H) \le 1$ is a function of the humidity, less than 1 if the humidity is lower than 80% (typically, the humidity inside a massive concrete structure such as a dam is included between 90 to 100%, although older ones may have a humidity in the range of 80 to 85%). $\dot{\xi}(t,\theta)$, the kinetics law, and latency time τ_{lat} and characteristic times τ_{car} are given by the following relation, illustrated by Fig. 1

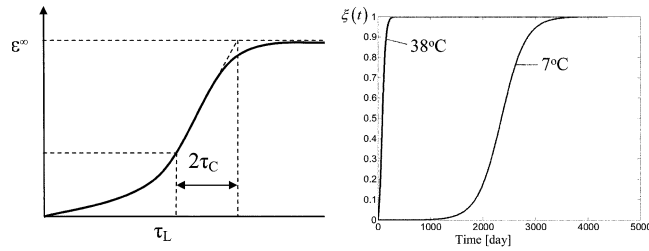

Fig. 1—Physical interpretation of parameters describing swelling evolution of AAR-affected concrete (Larive 1998). (Note: 38 °C = 100 °F; 7 °C = 44.6 °F.)

$$\xi(t,\theta) = \frac{1 - e^{-\frac{t}{\tau_C(\theta)}}}{1 + e^{-\frac{t-\tau_L(\theta, I_\sigma, f_c')}{\tau_C(\theta)}}};$$

$$\begin{cases} \tau_C(\theta) = \tau_C(\theta_0)\exp\left[U_C\left(\dfrac{1}{\theta} - \dfrac{1}{\theta_0}\right)\right] \\ \tau_L(\theta, I_\sigma, f_c') = f(I_\sigma, f_c')\tau_L(\theta_0)\exp\left[U_L\left(\dfrac{1}{\theta} - \dfrac{1}{\theta_0}\right)\right] \end{cases}$$

where θ is the current temperature, $\tau_L(\theta_0)$ and $\tau_C(\theta_0)$ are the reference latency and characteristic time measures in the laboratory at temperature θ_0, respectively. I_σ and f_c' are the first stress invariant and the concrete compressive strength, respectively. Finally, U_L and U_C are the activation energies for the latency and characteristic times.

Once the volumetric AAR strain is determined, it is decomposed into a tensorial strain in accordance to the three weight factors associated with the principal stresses (Saouma and Perotti 2006) and, as a result, the expansion is anisotropic.

Finally, the authors take into account a possible reduction in tensile strength and Young's modulus (which can be present along AAR expansion) by using the following temporal degradation expression

$$E(t,\theta) = E_0[1 - (1-\beta_E)\xi(t,\theta)];$$
$$f_t'(t,\theta) = f_{t,0}'\,[1 - (1-\beta_f)\xi(t,\theta)]$$

where E_0 and $f_{t,0}'$ are, respectively, the initial value of Young's modulus and tensile strength; β_E and β_f are, respectively, the residual fractional values of Young's modulus and tensile strength after AAR expansion; and $\xi(t,\theta)$ is the kinetic equation previously defined.

ANALYSES PROCEDURE

Whereas there may not be a remedy to AAR in most cases, engineers must have a numerical model that can predict the long-term structural response of the structure to anticipate potential structural deficiencies (such as cracks) and to properly plan remedial work.

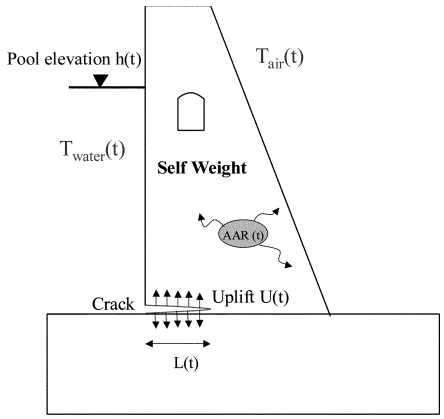

Fig. 2—Loads to be considered in analysis of dam affected by alkali-aggregate reaction.

As tempting as it may be, AAR can not be simply modeled as a mere equivalent thermal expansion with some limitation based on the corresponding stress. AAR is a thermodynamically-induced reaction (and hence depends on temperature), which is tightly coupled with the stress field (that can constrain expansion), and presence of cracks (that absorb the gel). By using the model previously presented by Saouma and Perotti (2006), this section will detail the analysis procedure for an AAR investigation.

Thermal analysis

Because of the temperature dependency, a transient thermal analysis of the structure must first be performed to obtain a temporal map of the internal temperature. For a dam, there is no need to model the rock base in such analysis. This requires a number of parameters, among them: 1) the air temperature variation (including the grouting temperature). In the reported analysis, the simplified model of Malla and Wieland (1999) was used; 2) the spatial (along the depth) and temporal (at least 12 or 24 increments a year) variation of the water temperature must be known. The model of Zhu Bofang (1985) for temperature depth variation was adopted; 3) the pool elevation variation during a typical year must also be known as it affects the state of stress; and 4) the concrete thermal properties must also be determined. For this analysis, and the subsequent stress one, an analysis time unit (ATU), or time increment, is defined.

Stress analysis

Following the transient thermal analysis, the stress analysis can be performed, and an effective E is used to account for long-term creep ($E_{ff} = E_i/(1 + c_t)$, where c_t is the specific creep coefficient and E_i is the initial modulus. It should be noted, however, that the finite element mesh for the stress analysis of a dam affected by AAR has to be different from the one used for the thermal analysis and it includes the joints, the interface between dam and rock foundation, and the rock foundation. These parts are not necessary in the thermal analysis but are very important to capture the real behavior of a dam affected by AAR (and thus to capture the real crest displacements on which parameter identification is based as explained in the following paragraph). Indeed, AAR expansion can result in: 1) opening of the vertical joints downstream and closure of the vertical joints upstream in an arch dam; 2) possible movement of the different buttresses of a gravity dam along the joints; and 3) sliding of the dam subjected to a compressive state of stress on the foundation joint.

With regard to the temporal and spatial variation of the temperature, it should be kept in mind that the stress analysis requires the temperature difference with respect to the stress-free temperature (namely, the ambient air temperature during grouting $\theta(x, y, z) - \theta_{grouting}$, whereas the AAR evolution depends on the total absolute temperature inside the dam $\theta(x, y, z)$.

Loading definition for an AAR investigation can be quite complex and error prone (unless it is fully automated) (Fig. 2). The impounding of the newly completed dam is first simulated through a few increments (approximately five) to allow joint adjustments in the nonlinear analysis where nonlinearity of the joints is modeled by a special interface element (Cervenka et al. 1998). Following this initial phase, and taking into account the dam completion data to perform a reliable analysis and future prediction, the analysis input data file is completed as follows. For each of the n years (typically 50), and for each of the m yearly ATUs (typically 24 per year; each time increment corresponds to approximately 2 weeks), apply correct pool elevation (upstream and downstream), uplift pressures, and internal nodal temperatures. This can result in a three-dimensional analysis in a 500 MB input data file.

Analysis and data preparation for this investigation were performed by using a specially modified finite element code (Merlin 2006) and finite element preprocessor (Kumo 2006).

System identification

A particularly challenging problem in the analysis of older structures affected by AAR is the determination of the kinetics parameters (ε^{∞},$\tau_L(\theta_0)$, and $\tau_C(\theta_0)$). The difficulty stems from the fact that one is confronted (almost by definition) with older structures for which it is practically impossible to conduct laboratory experiments and extract an expansion curve. Hence, the structural analysis must be conducted with an initial set of assumptions, results compared with the dam recorded displacements, and then input parameters updated. This labor- and computation-intensive procedure is prone to numerous errors and is inefficient. Accordingly, AAR problems are prime candidates for system identification.

Mathematically, the problem can be simply formulated as follows. The field recorded (usually crest) displacements are denoted by $u(t)$, the kinetic (and possibly other) parameters as x, and the finite element operator $f(.)$, and computed results by $u(t, x)$. Hence, $f(x) = u'(t, x) \neq u(t)$. The authors seek to minimize the objective function $\omega(x)$ defined as follows along with the Jacobian, Gradient, and Hessian matrixes (Dennis and Schnabel 1983)

$$\omega(x) = (u - u')^T(u - u') = r^T \cdot r = \sum_{i=1}^{m} (u_i - u_i')^2;$$

$$J(x) = \frac{\partial r(x)}{\partial x^T} = \frac{\partial}{\partial x^T}[(u - u')] = \frac{\partial u}{\partial x^T} - \frac{\partial u'}{\partial x^T} = -\frac{\partial u'}{\partial x^T} = -L$$

$$\nabla\omega(x) = \frac{\partial \omega(x)}{\partial x^T} = \frac{\partial}{\partial x^T}[(u - u')^T(u - u')] = 2J^T r;$$

$$H(x) = \frac{\partial^2 \omega}{\partial x^T \partial x} = \frac{\partial}{\partial x}(\nabla\omega(x)) = \frac{\partial}{\partial x}[2J^T r] = 2J^T J + 2\frac{\partial^2 r}{\partial x^T \partial x} r$$

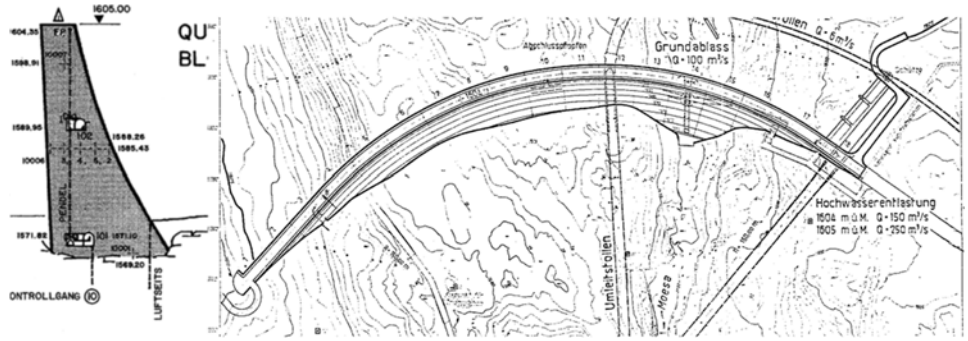

Fig. 3—Arch gravity dam geometrical layout.

Near the minimum, $((\partial^2 r)/(\partial x^T \partial x))r \to 0$, then $H(x) = 2J^T J$. Using the Levenberg-Marquardt method (Dennis and Schnabel 1983), x_{k+1} from $x_{k+1} = x_k - [\varepsilon_k I + H(x_k)]^{-1}\nabla\omega(x_k)$ where $\varepsilon_k > 0$ is such that all the eigen values of $[\varepsilon_k I + H(x_k)]$ are greater than $\delta > 0$. Finally, the authors used a development of the Levenberg-Marquardt method: the trust region method. The authors tried to minimize the objective function $\omega(x)$ inside a trust region where the quadratic approximation, obtained by Taylor series, is considered reliable

$$\omega_{II}(x, x_k) = \omega(x_k) + \nabla\omega(x_k)^T(x - x_k) + \frac{1}{2}(x - x_k)^T H(x_k)(x - x_k)$$

The trust region is defined as follows

$$\Omega_k = \{x: \|x - x_k\| \le \Delta_k\}; \ \Delta_k > 0$$

and the optimization problem becomes $min_x\{\omega_{II}(x, x_k): x_k \in \Omega_k\}$. The condition to update the region is given by

$$R_k = \frac{\omega(x_k) - \omega(x_{k+1})}{\omega(x_k) - \omega_{II}(x_{k+1})} \cong 1$$

The update of the starting point is the same illustrated for the Levenberg-Marquadt method.

Finally, in this method the upper and lower bounds for the parameters can also be defined as

$$min_x\{\omega_{II}(x, x_k): x_k \in \Omega_k\}; \ (\boldsymbol{l_b} \le x \le \boldsymbol{u_b})$$

From a practical point of view, the following three considerations must be accounted for in the optimization process:

The starting point of the parameter identification may be determined from laboratory tests (from which a first estimate of $\varepsilon^{\infty}\big|_{\theta = \theta_0}$, $\tau_L(\theta_0)$, and $\tau_C(\theta_0)$ can be obtained). Alternatively, curve fitting of the dam crest displacement

$$u_{irr}^{AAR}(t, \theta) = \frac{1 - e^{-\frac{t}{\tau_C(\theta)}}}{1 + e^{-\frac{t - \tau_L(\theta, I_\sigma, f_c')}{\tau_C(\theta)}}} u_{irr}^{AAR, \infty}$$

(where $u_{irr}^{AAR, \infty}(t, \theta)$ and $u_{irr}^{AAR, \infty}$ are the time- and temperature-dependant irreversible displacement and the final displacement due to AAR, respectively) one may make a prudent guess for the times, but not for $\varepsilon^{\infty}\big|_{\theta = \theta_0}$.

The sought parameters must be normalized such that all the initial values have the same order of magnitude: a) the initial variation must be large enough to produce a variation of the computed results (large normalized values can lead to an immediate stop of the identification program); and b) the final variation of the parameters must be small enough to permit a small final adjustment of the identified parameters without large oscillation around the final solution (if the normalized parameter is too small, it may result in large final oscillation).

A weight function can be used to assign importance to the last data field which usually have a major absolute value and thus better represent the irreversible effect of the AAR expansion with respect to the effect of normal loads. It should be noted that this system identification does not require a thermal analysis and, from a practical point of view, entails a simple modification of three variables in the stress analysis input file.

TWO-DIMENSONAL PARAMETRIC STUDY

Given the relative complexity of the analysis procedure, and before undertaking a three-dimensional analysis, it was deemed desirable to perform a preliminary two-dimensional parametric analysis to address the following questions: 1) How does AAR affect the state of stress in a dam subjected to normal gravity (G), hydrostatic (H), and temperature (T) loads? 2) Should the seasonal variation in pool elevation and in temperature during a long-term analysis of a dam subjected to AAR be accounted for? 3) How many increments per year are necessary to obtain reliable results? 4) Is it important to model the dam/foundation joint in an AAR analysis? 5) How important is it to model the sigmoid kinetics? 6) How important is the effect of concrete Young's modulus degradation? 7) Is it important to model the internal and external concrete of a dam, which have different cement contents and, thus, alkali content? and 8) How different is the authors' model from the one of the state of the practice? As a vehicle for this preliminary investigation, a two-dimensional model of the three-dimensional analyzed arch gravity dam (Fig. 3) is adopted.

Due to the complex interplay among temperature, stresses, and expansion, the internal core of the dam (being cooler because it is not directly exposed to outside fluid and, hence, with a reduced expansion) constrains the expansion of the external layer, which produces tensile stresses in the inner part. This may give rise to hidden (except in the gallery) internal structural cracks. The potential for internal cracking can also be visualized through the stress distribution between the dam and the rock. As shown in Fig. 4, there is an intermediary zone of both high tensile stresses along the base, and upward displacement along the central core. As a result of

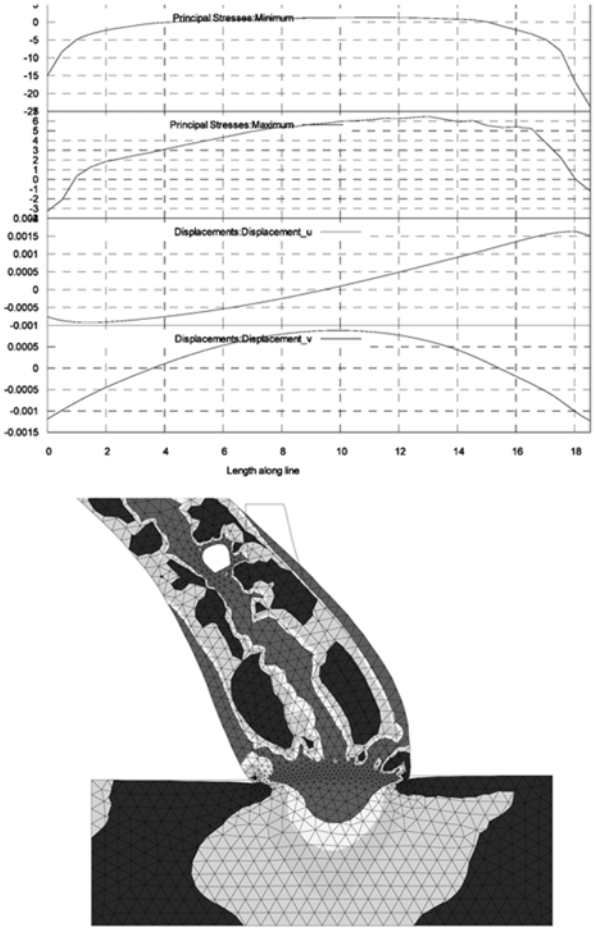

Fig. 4—Minimum/maximum stresses (MPa) and displacements (m) along rock/concrete rigid interface; maximum principal stresses (MPa) and deformation of dam. (Note: 1 MPa = 0.145 ksi).

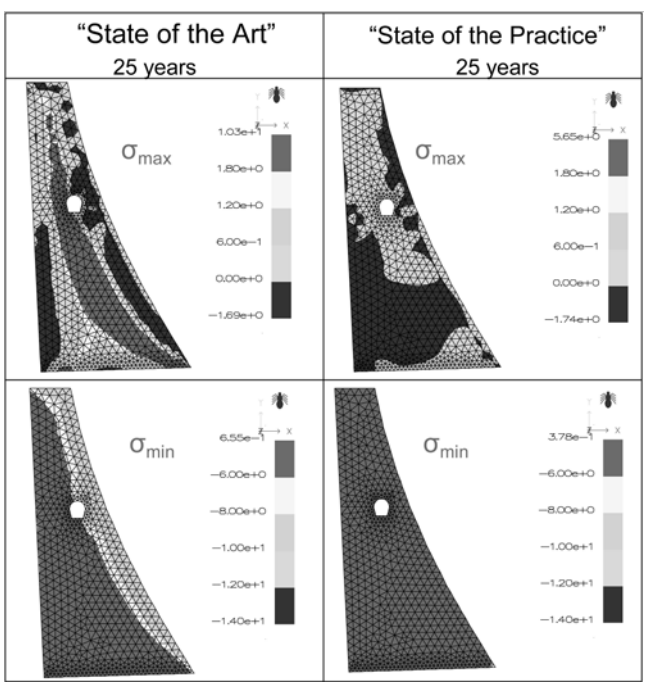

Fig. 5—Proposed state-of-the-art model versus state-of-the-practice model (principal stresses in MPa). (Note: 1 MPa = 0.145 ksi.)

this, in subsequent analyses, joint elements were placed between the rock and the concrete.

The proposed model (Saouma and Perotti 2006) was compared with the state-of-the-practice model. Both models were calibrated to yield the same crest displacement after 50 years (as made in practice to calibrate an analysis); however, the former assumed the sigmoid expansion curve, and the latter a linear one. Comparing the two internal maximum stresses (Fig. 5), it is clear that the state-of-the-practice model is greatly underestimating the magnitude of the tensile stresses (as compared with the authors' model). This can be attributed to the lack of AAR strain redistribution (ability to transform a volumetric AAR strain into principal AAR strains along the principal stresses) in that model, as well as the lack of thermal sensitivity of the model.

Finally, and with regard to the other original objectives of this preliminary parametric study, it was determined (due to space limitation not all results were explicated) that: 1) AAR causes a bulging in the displacement and tension in the center. This is important as it may cause internal unnoticeable cracks and may explain the cracks observed inside the gallery of the analyzed dam as explained in the following paragraphs; 2) the temperature temporal variation must be modeled; 3) hydrostatic/uplift load is important only to assess failure; effect on AAR-induced response is minimal (its activation does not alter the stress field sufficiently to affect the expansion). Hydrostatic/gravity/thermal minimum stresses are approximately 3 MPa (435.11 psi), whereas AAR results in a total minimum stress of approximately 14 MPa (2030.53 psi). For dams above 50 m (164 ft), however, they should be included in all analyses; 4) must use 12 or 24 increments per year to correctly capture the effects of temperature variation; 5) foundation/dam interface and dam joints must be modeled; 6) the state-of-the-practice model, when calibrated to yield same displacements as Saouma and Perotti (2006), yields stresses that are lower (and, hence, potentially unconservative); 7) it is usually not important to model Young's modulus degradation (degradation had little effect on long-term crest displacement). In any case, it is very difficult to properly estimate the final value of the Young's modulus (in this parametric study, a degradation equal to 30% was assumed based on pessimistic experimental data available for existing dams [Health ACRES 2006; Cavalcanti et al. 2000]); and 8) there is no need to model inner and external concrete separately.

Arch gravity dam analysis

Following the two-dimensional parametric analysis, the three-dimensional analysis was conducted. The initial mesh is shown in Fig. 6. As a result of the initial two-dimensional parametric study, key analysis parameters were identified, and this final analysis encompassed three parts: 1) thermal analysis of a mesh without the joints and the rock foundation; 2) parametric identification study of the dam up to 1997; and 3) final predictive analysis using the AAR parameters $\tau_L(\theta_0)$, $\tau_C(\theta_0)$, and $\varepsilon_{\theta_0}^{\infty}$ identified in the previous analysis. Despite the coarser mesh, and an ATU of 1 month, the computed internal temperature map was almost identical to the one obtained from the two-dimensional analysis with a finer mesh and with 1 ATU equal to 2 weeks.

Parameter identification and analysis results

Of paramount importance to the long-term reliable prediction of the dam response is the ability of the model to also simulate

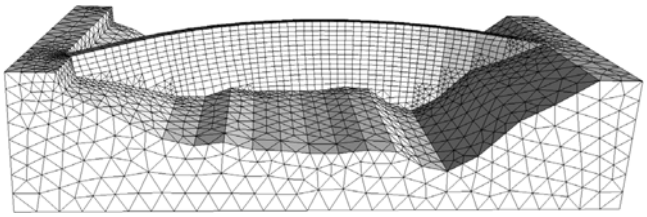

Fig. 6—Three-dimensional mesh.

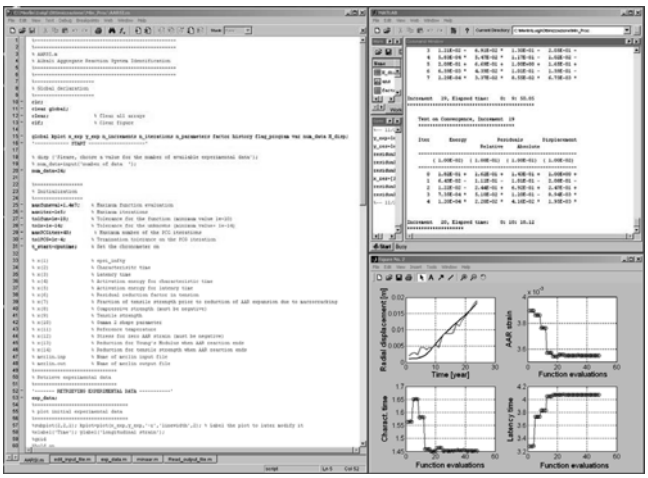

Fig. 7—Graphical user interface for AAR parameter identification.

the past response. In a dam, there is always a record of the crest irreversible displacement with time; it is precisely this curve that a model should be able to duplicate as well as possible. Hence, using the approach previously described, a driver program was written to identify the three key parameters $\varepsilon^{\infty}\big|_{\theta=\theta_0}$, $\tau_L(\theta_0)$, and $\tau_C(\theta_0)$ by continuously comparing the histogram of crest displacement computed with the one recorded. The driver will: 1) launch an initial finite element analysis; 2) open the output file and extract the crest displacement histogram; 3) compare the numerical histogram with the field recorded one. If results are nearly similar (the established convergence is reached), stop execution; and 4) appropriately modify the input key parameters and launch the finite element analysis. This procedure is best illustrated by Fig. 7 where left—driver program code; upper right—finite element analysis program execution; lower right—comparison of computed and recorded crest displacement (upper left) and variation of $\tau_L(\theta_0)$, $\tau_C(\theta_0)$, and $\varepsilon_{\theta_0}^{\infty}$ versus iterations.

Figure 8 shows that the computed crest displacement is well within the seasonal variations of the numerical final predictions. Hence, having validated the model with measurements made up to 1997, a single, final analysis was conducted up to 2020. It was determined that the expansion should stop around 2010 (expansion data subsequent to 1995 were not made available to the authors).

For the three-dimensional mesh (7552 nodes and 5196 elements), the total identification procedure took approximately 190 hours on a computer. Figure 9 shows the internal AAR-induced maximum principal stresses. The maximum principal stress field inside the dam can explain the cracks discovered along the upper gallery of the analyzed dam.

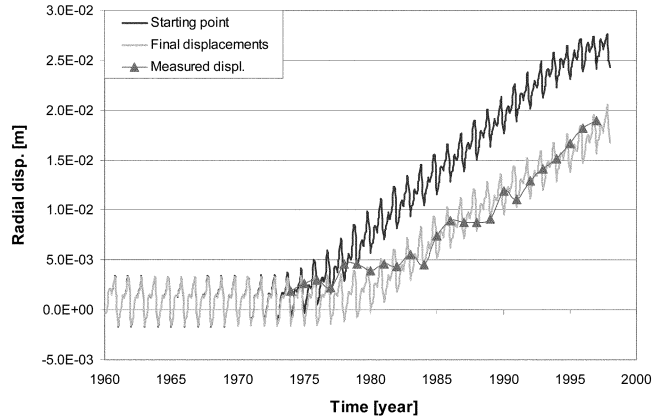

Fig. 8—Comparison between first guess analysis and final analysis with optimized parameters. (Note: 1 m = 33 in.)

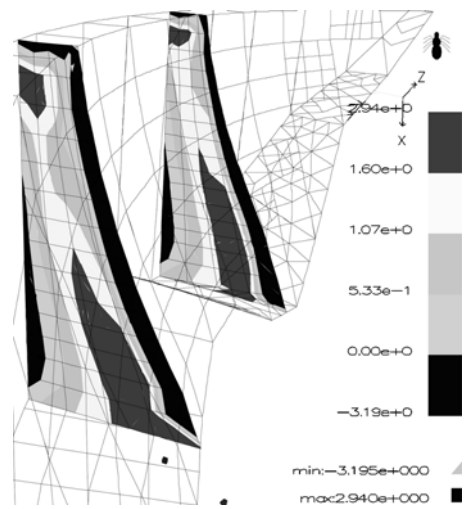

Fig. 9—Internal AAR-induced maximum principal stresses (MPa). (Note: 1 MPa = 0.145 ksi.)

HOLLOW BUTTRESS DAM ANALYSIS

This second example is drawn from the contribution of the authors to the Eighth ICOLD Benchmark Workshop on Numerical Analysis of Dams in which contributors were asked to assess the safety of Poglia Dam (Saouma et al. 2005). The dam (Fig. 10) is a hollow-gravity dam composed of two lateral gravity dams and four hollow diamond-head-buttress central elements.

It is characterized by a crest length of 137.1 m (450 ft), a height of 50 m (164 ft), two 14 m (46 ft) wide spillways, and joint spacing of 22 m (72 ft). The base, maximum, and operating pool elevations are 628.1, 632, and 625 to 628 m (2060, 2073, and 2050 to 2060 ft), respectively. Accelerated laboratory expansion tests were conducted on cores (extracted from Poglia Dam) at both 38 and 80 °C (100 and 176 °F). From these tests, it was estimated that the residual expansion is approximately 0.95×10^{-3}.

Whereas there is no chart plotting the crest displacement with time, it is understood that the crest vertical drift, started in 1970, reached 8 mm (0.31 in.) in 1982, and then reached a total value of 30 mm (1.18 in.) in 2000. The increase was quasi-linear with a slight increase in rate in the later years. In addition, an irreversible displacement of approximately 0.1 and 0.2 mm/year (0.004 and 0.008 in./year) was recorded in the cross-valley direction (toward the right), and along the

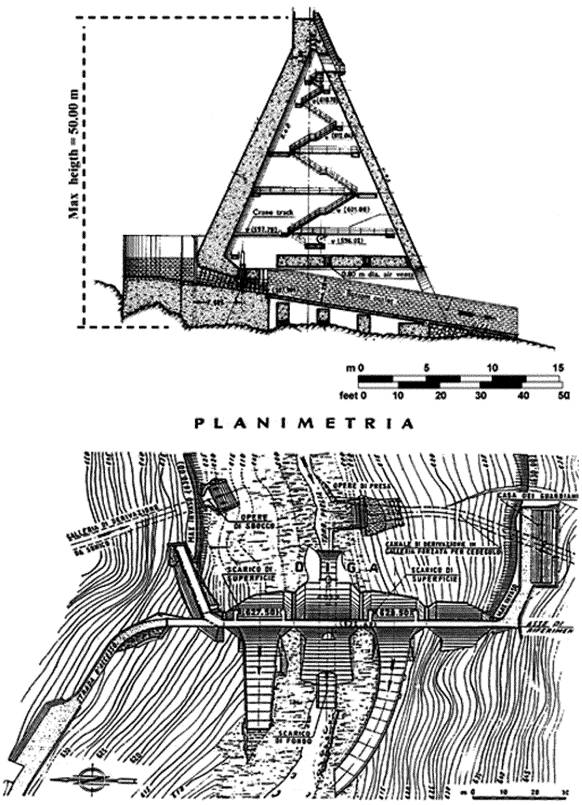

Fig. 10—Section (central element) and plan of Poglia Dam.

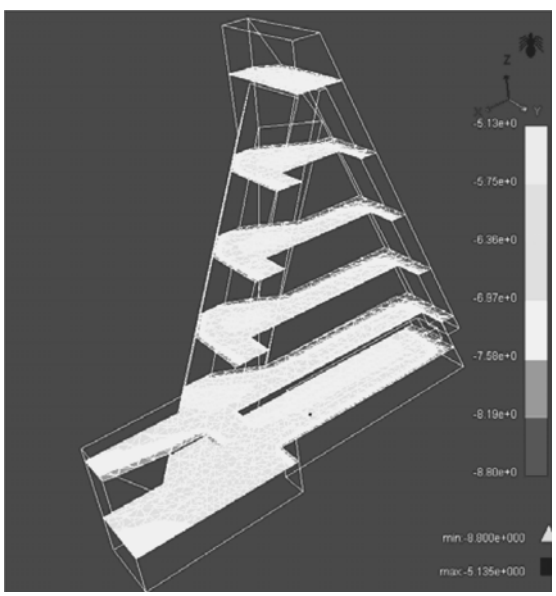

Fig. 11—Internal temperature of Poglia Dam. (Note: 1 °F = 9/5 °C + 32.)

stream direction, respectively. Finally, and what may be most worrisome, a downstream displacement of the right corner was recorded (due to the lateral expansion of the two adjacent blocks).

Transient thermal analysis

As the authors' AAR model was highly dependant on the temperature, a preliminary transient thermal analysis was performed. In this analysis, only the dam was considered. Half the central element was modeled, and due to symmetry, adiabatic boundary conditions were applied on the plane of symmetry. Convection was ignored, and recorded temperatures were applied on those faces exposed to air (outside and inside) and to water.

The conductivity k was set to 10.12 kJ/(m hr °C (715 kW/in. °F) and the mass density to 2431 kg/m^3 (150 lb/ft^3). Transient analysis was performed for 5 years, and because results stabilized after 4 years, the results of the fifth year were considered representative of the yearly temperature variation. Figure 11 shows the internal temperature inside the dam.

Table 1—AAR properties

		Initial	Final
Maximum volumetric strain	$\varepsilon^{\infty}\big\vert_{\theta=\theta_0}$	1.81×10^{-3}	3.50×10^{-3}
Characteristic time	$\tau_C(\theta_0)$	77.1 ATU	60 ATU
Latency time	$\tau_L(\theta_0)$	476.5 ATU	160 ATU
Actual energy for characteristic time	U_C	5400 K	
Actual energy for latency time	U_L	9400 K	
Fraction of tension	g_t	0.8	
Maximum compressive strength	f_c'	–32.0 MPa (–4640 psi)	
Maximum tensile strength	f_t'	1.5 MPa (217.5 psi)	
Coefficient	β	0.5	
Reference test temperature	θ_0	11.8 °C (53.2 °F)	
Sigma 2	σ_U	–10 MPa (–1450 psi)	

Stress analysis

Following the thermal analysis, a stress analysis was conducted using a mesh that included dam, foundation, and interface joints between the rock and concrete. Material properties adopted in the analysis are those specified by the Benchmark Workshop with one notable exception. The tensile strength and the cohesion of the dam/foundation interface were increased to 1.5 and 1.0 MPa (217 and 145 psi) (rather than the specified 0.15 and 0.10 MPa [21.8 and 14.5 psi] specified) because preliminary analysis indicated that those values were too small to resist the pool elevation. The initially selected AAR properties and the final ones determined through minimization are shown in Table 1. It should be noted that only an initial guess on the maximum volumetric strain latency and characteristic time was made, as those were subsequently to be determined from an automated system identification procedure. Following convergence of this minimization (of the error between computed and measured crest displacements), further fine-tuning was performed manually to further reduce that error. The final (numerically obtained) volumetric strain was 3.50×10^{-3}, whereas the experimentally obtained one (from laboratory tests) was 0.95×10^{-3}; however, total expansion of the dam could only be justifiably determined from the numerical one.

Gravity load (dam only) was applied in the first increment and the displacements (but not the stresses) were subsequently reset to zero (to eliminate self-weight displacements from the results). Subsequently, the pool elevation was raised from a base elevation of 582.10 m (1909 ft) to a maximum elevation of 628.09 m (2060 ft) in four increments of 11.5 m. (37.7 ft) each. It should be noted that as the pool elevation was raised, not only did it increase the hydrostatic pressure, but also the uplift pressure distribution under the dam. This pressure distribution will be automatically adjusted from a triangular one to a trapezoidal one should the dam base crack. From the sixth

increment onward, the pool elevation was kept constant, and the AAR was active (increments six and seven correspond to the winter and summer of the first year). An analysis corresponding to the 55 years of dam operations was made, and the resulting crest displacements compared with the measured ones.

Results

The three-dimensional finite element mesh had 6145 nodes and 24,133 elements. The three-dimensional nonlinear analysis used the tangent stiffness method along with line search and entailed 115 increments. Convergence criteria were set to 0.01, 0.02, 0.05, and 0.02 for the energy, relative residual (ratio of the Euclidian norm of the current and initial residual load vectors), absolute residual (ratio of the infinity norm of the current and initial residual load vectors), and displacement error, respectively. A maximum of 50 iterations was allowed. Each analysis took approximately 7 hours on a 3.00 GHz processor with 1.5 GB of RAM.

Figure 12 shows the vertical and horizontal crest displacements. The following observations can be made: 1) the final maximum crest vertical displacement is approximately 30 mm (1.18 in.); 2) the seasonal variation of the displacements is nonnegligible compared with the total AAR irreversible one; and 3) the kinematics of the displacement is not yet satisfactorily captured (Fig. 12). Yet, this may be partially due to the scarcity of field observations (and there is no indication if they were taken in the summer or winter) and to the fact that the lateral and significant dam displacement/sliding is ignored; and 4) the horizontal displacements are substantially smaller than the vertical displacement due to the lateral constraints.

The overall deformed shape is puzzling (Fig. 13). It appears that for the given numerical assumptions, most of which were stipulated by the Benchmark Workshop organizers, the dam is failing through sliding. The sharp curvature of the deformation at the top corresponds to the pool elevation, which is indeed 2 m (6.6 ft) below the crest.

Figure 14 illustrates various contour lines for the main rock/concrete joint. Interestingly, it is noted that the crack-opening displacements are maximum in the middle and minimum on the upstream/downstream side. This was already observed in the arch gravity dam previously analyzed. Normal stresses are mostly zero, and the full uplift develops over most of the joint. The joint sliding displacement is linear and is, at most, equal to 45 mm (1.77 in.) (adoption of the line search method may have constrained the overall sliding to such a small value). Also shown is the shear distribution over the joint. The overall AAR expansion at the end of the analysis ε^{∞} was 1.65×10^{-3} whereas actual AAR expansion inside the dam was approximately 4×10^{-4}. The difference was caused by the reduction factors of the model. Furthermore this expansion is, on average, equivalent to 40 °C (104 °F), which is just slightly cooler than the 42 °C (108 °F) determined in a previous study in which the interface was not modeled, and the thermal expansion was uniform (Saouma and Perotti 2004).

A second analysis was conducted with the lateral sides of the dam unconstrained in the lateral (Z) direction. Figure 15 shows that with the lateral sides of the dam free to expand, the vertical displacement reduced in accordance with the premises of the model. Finally, Fig, 16 is a mere speculation on the likely mode of failure mechanisms of this dam if a full three-dimensional analysis were to be undertaken. The sharp corner between the two dam segments constitutes herein the dam's Achilles' heel. This worrisome aspect warrants further investigation.

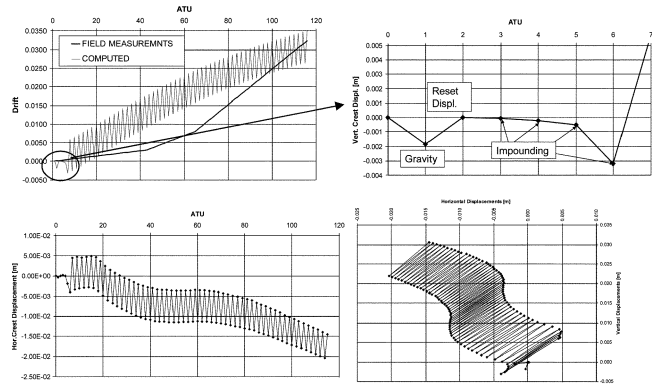

Fig. 12—Crest vertical and horizontal displacements versus ATU; vertical versus horizontal displacements. (Note: 1 m = 39.37 in.)

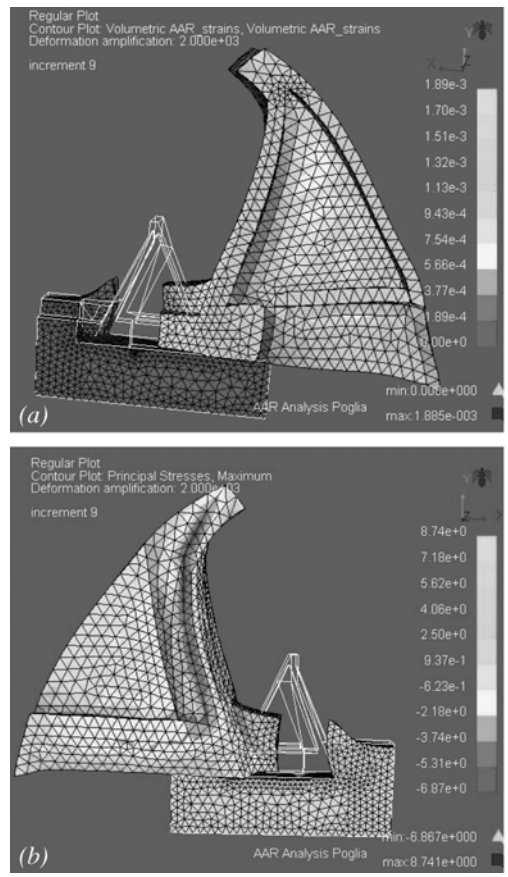

Fig. 13—Deformed shape with contour plot of volumetric AAR strain (a); and maximum principal stresses (MPa) (b). (Note: 1 MPa = 0.145 ksi.)

MAJOR REINFORCED CONCRETE STRUCTURE

The last example investigated is the effect of AAR expansion in a massive reinforced concrete structure that supports a high-voltage transmission tower (Fig. 17). The cross girder and the column are 1.5 x 1.5 m and 2.0 x 2.0 m (4.9 x 4.9 ft and 6.56 x 6.56 ft), respectively, in cross section, and the span is 13.7 m (45 ft). The girder is heavily reinforced: 1) longitudinally 14ϕ29 (1.14 in) and 14ϕ22 (0.97 in.); and 2) vertically ϕ16 (0.62 in.) spaced at 250 mm (9.84 in.). An unusual crack pattern was observed, and AAR expansion was suspected. This was later confirmed by laboratory tests and preliminary finite element analysis was conducted to improve under-

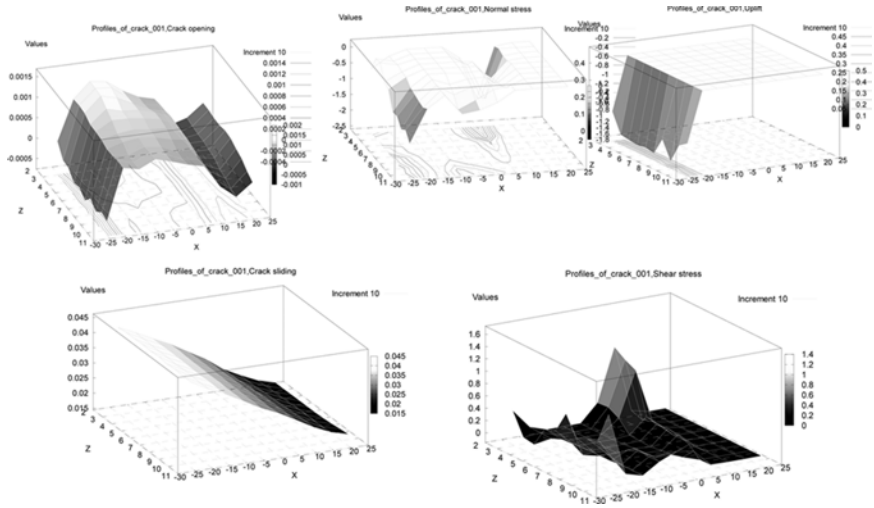

Fig. 14—Contour plots of main rock/concrete joint; joint opening displacements (m), normal stresses (MPa), uplift pressures (MPa), joint sliding displacements (m), and joint shear stresses (MPa). (Note: 1 MPa = 0.145 ksi).

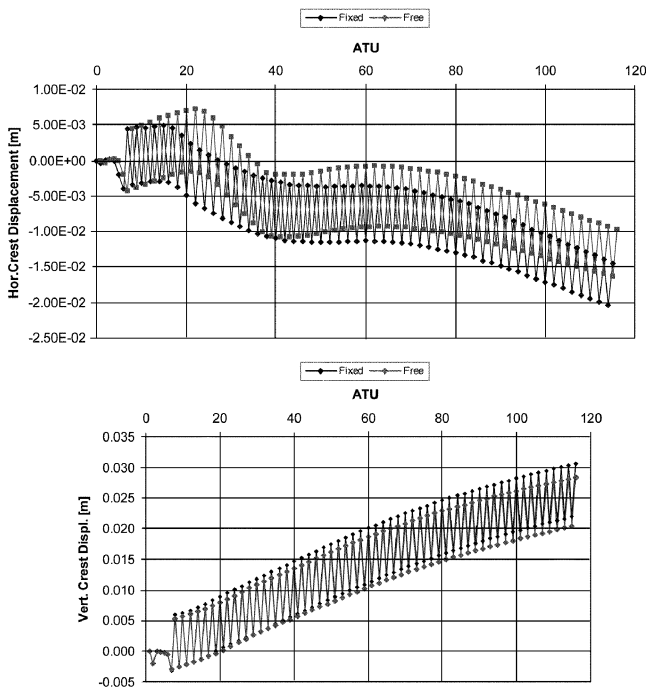

Fig. 15—Effect of lateral constraints on AAR expansion. (Note: 1 m = 39.37 in.)

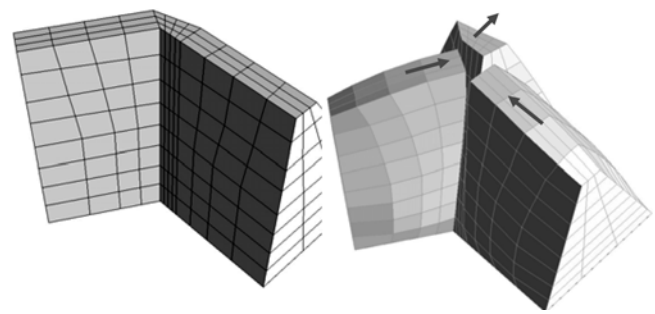

Fig. 16—Possible failure mechanism at joint connecting two parts of dam.

Fig. 17—AAR-affected reinforced concrete structure supporting high voltage transmission tower.

standing of the structural response and anticipate possible future remediation.

A single frame of the structure was modeled through a three-dimensional mesh and was analyzed with the model previously described. Contrary to dams where it was reasonable to assume that the humidity was sufficiently high to enable the AAR reaction, this assumption may no longer be valid for this structure. In this preliminary analysis, however, the effect of humidity variation was neglected and left for future studies. Furthermore, this preliminary study attempted simply to qualitatively explain the crack formations.

Following a 50-year simulation (Fig. 18), it was observed that zones of high tensile stresses do indeed correspond to the location of the observed cracks in the field. The high tensile zone, however, seems to be isolated to the external part of the concrete beam; thus, the observed cracks can be only superficial. Furthermore, as anticipated, the AAR expansion causes high compressive and tensile stresses with respect to the initial case where only dead loads are considered; this may require a further nonlinear analysis of this structure. Finally, the AAR strain distribution inside the girder is highly dependent on the presence of compressive stresses as dictated by the model.

CONCLUSIONS

AAR engineering simulation is of paramount importance to engineers confronted with a degraded structure. The most important questions are how long will the structure continue

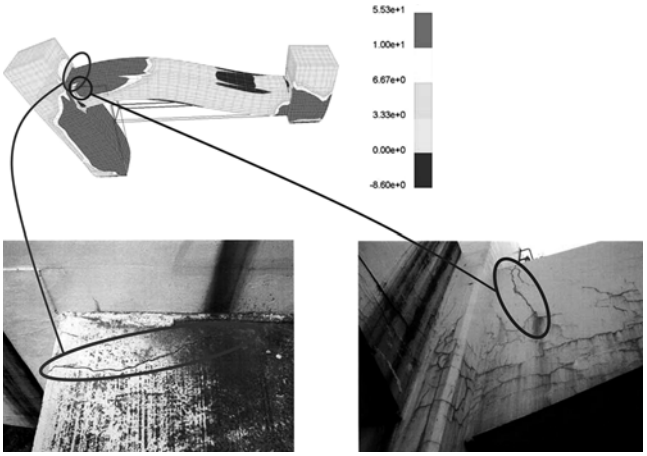

Fig. 18—Correlation between AAR finite element simulation and observed cracks.

to expand (given constant exposure to the reactive alkali and aggregates), and what would be the accompanying structural response. This study presents a rigorous procedure, largely based on the model of the first two authors (Saouma and Perotti 2006) that accounts for thermal and load time fluctuations. It would typically entail a preliminary transient thermal analysis to be followed by a system identification procedure if field measurements are available. The viability of the methodology was illustrated through the analysis of three different structures. To the best of the authors' knowledge, this is the most comprehensive analytical methodology to investigate AAR-affected structures thus far (based on the realism of the investigated structures), and will hopefully stimulate further research and applications in this direction.

ACKNOWLEDGMENTS

Development of the AAR model and the first analysis were made possible through the financial support of the Swiss Federal Office of Water and Geology (DFEG). The last two analyses were supported by the Tokyo Electric Power Company.

REFERENCES

Ahmed, T.; Burley, E.; and Rigden, S., 1998, "The Static and Fatigue Strength of Reinforced Concrete Beams Affected by Alkali-Silica Reaction," *ACI Materials Journal*, V. 95, No. 4, July-Aug., pp. 376-388.

Bangert, F.; Kuhl, D.; and Meschken, G., 2004, "Chemo-Hygro-Mechanical Modelling and Numerical Simulation of Concrete Deterioration Caused by Alkali-Silica Reaction," *International Journal of Numerical Analysis and Methods of Geomechanics*, V. 28, pp. 689-714.

Cavalcanti, A. J.; Silveira, A. M.; and Degaspare, J. C., 2000, "AAR Management at Paulo Afonso IV Power Plant—Brazil," *11th International Conference on Alkali-Aggregate Reaction*, Quebec, Canada, pp. 1262-1272.

Cervenka, J.; Chandra, J. M.; and Saouma, V., 1998, "Mixed Mode Fracture of Cementitious Bimaterial Interfaces; Part II: Numerical Simulation," *Engineering Fracture Mechanics*, V. 60, No. 1, pp. 95-107.

Charlwood, R. G.; Solymar, S. V.; and Curtis, D. D., 1992, "A Review of Alkali Aggregate Reactions in Hydroelectric Plants and Dams," *Proceedings of the International Conference of Alkali-Aggregate Reactions in Hydroelectric Plants and Dams*, Fredericton, New Brunswick, Canada, pp. 1-29.

Dennis, J. E., and Schnabel, R. B., 1983, *Numerical Methods for Unconstrained Optimization and Nonlinear Equations*, Prentice-Hall, Englewood Cliffs, N.J., 394 pp.

Fan, S., and Hanson, J., 1998, "Length Expansion and Cracking of Plain and Reinforced Concrete Prisms due to Alkali-Silica Reaction," *ACI Materials Journal*, V. 95, No. 4, July-Aug., pp. 480-487.

Gilks, P., and Curtis, D., 2003 "Dealing with the Effects of AAR on the Water Retaining Structures at Mactaquac GS," *Proceedings of the 21st Congress on Large Dams*, Montreal, Quebec, Canada, pp. 681-703.

Gomes, J. P.; Batista, A. L.; and Oliveira, S., 2004, "Analysis of Concrete Dams Under Swelling Processes," *12th International Conference on Alkali-Aggregate Reaction in Concrete*, pp. 1148-1157.

Hatch ACRES Corp., 2006, http://www.hatchacres.com/Company/Services/ServHydroAAR/indcnt.htm.

Huang, M., and Pietruszczak, S., 1999, "Alkali-Silica Reaction: Modeling of Thermo-Mechanical Effects," *Journal of Engineering Mechanics*, ASCE, V. 125, No. 4, pp. 476-487.

ICOLD, 2001, "Numerical Analysis of Dams," *Proceedings of the Sixth ICOLD Benchmark Workshop*, Salzburg, Austria.

Jabarooti, M. R., and Golabtoonchi, I., 2003, "Alkali-Aggregate Reactivity in South-East Iran," *Proceedings of the 21st Congress on Large Dams*, Montreal, Quebec, Canada, pp. 53-62.

Jones, A. E. K., and Clark, L. A., 1996, "The Effects of Restraint on ASR Expansion of Reinforced Concrete," *Magazine of Concrete Research*, V. 48, No. 174, pp. 1-13.

Kumo, 2006, "Finite Element Preprocessor for Merlin," *Tokyo Electric Power Company Internal Report*, http://ceae.colorado.edu/~saouma/kumo.

Larive, C., 1998, "Apports Combinés de l'Experimentation et de la Modelisation à la Comprehension de l'Alcali Reaction et de ses Effects Mecaniques," Laboratoire Central des Ponts et Chausses (LCPC), Paris, France.

Li, K., and Coussy, O., 2002, "Concrete (ASR) Degradation: from Material Modeling to Structure Assessment," *Journal of Concrete Science and Engineering*, V. 4, pp. 35-46.

Malla, S., and Wieland, M., 1999, "Analysis of an Arch-Gravity Dam with a Horizontal Crack," *Computers and Structures*, No. 72, pp. 267-278.

Merlin, 2006, "Finite Element Analysis Program," *Tokyo Electric Power Company Internal Report*, http://ceae.colorado.edu/~saouma/merlin.

Mohammed, T. U.; Hamada, H.; and Yamaji, T., 2003, "Alkali-Silica Reaction-Induced Strains over Concrete Surface and Steel Bars in Concrete," *ACI Materials Journal*, V. 100, No. 2, Jan.-Feb., pp. 133-142.

Monette, L. J.; Gardner, N. J.; and Grattan-Bellew, P. E., 2002, "Residual Strength of Reinforced Concrete Beams Damaged by Alkali-Silica Reaction—Examination of Damage Rating Index Method," *ACI Materials Journal*, V. 99, No. 1, Jan.-Feb., pp. 42-50.

Multon, S.; Seignol, J. F.; and Toutlemonde, F., 2005, "Structural Behavior of Concrete Beams Affected by Alkali-Silica Reaction," *ACI Materials Journal*, V. 102, No. 2, Mar.-Apr., pp. 67-76.

Murtaugh, B. R., 1995, "Beltzville Dam Intake Tower Alkali-Silica Reaction, A Case Study," *Final Report of a Term Project for Advanced Concrete Technology I*, Drexel University, Philadelphia, Pa.

Nuss, L., 2005, personal communication, U.S. Bureau of Reclamation.

Portuguese National Committee on Large Dams, 2003, "Ageing Process and Rehabilitation of the Pracana Dam," *Proceedings of the 21st Congress on Large Dams*, Montreal, Quebec, Canada, pp. 121-138.

Saouma V. E., and Perotti, L. E., 2004, "Analisi dell'Elemento Centrale Della Diga del Poglia con il Programma MERLIN," *Report*, submitted by Politecnico of Milan to CESI.

Saouma, V. E., and Perotti, L. E., 2005, "State of the Art Survey of Alkali Aggregate Reactions in Reinforced and Massive Concrete," *Technical Report*, submitted to the Tokyo Electric Power Service Company.

Saouma, V. E., and Perotti, L. E., 2006, "Constitutive Model for Alkali Aggregate Reactions," *ACI Materials Journal*, V. 103, No. 3, May-June, pp. 194-202.

Saouma, V. E.; Perotti, L.; and Uchita, Y., 2005, "AAR Analysis of Poglia Dam with Merlin," *Eighth ICOLD Benchmark Workshop on Numerical Analysis of Dams*, Wuhan, China.

Sinclair, M., and Wark, R., 2003, "Canning Dam Remedial Works, Australia's Largest Permanent Ground Anchors," *Proceedings of the 21st Congress on Large Dams*, Montreal, Quebec, Canada, pp. 155-172.

Thompson, G. A.; Charlwood, R. G.; Steele, R. R.; and Curtis, D. D., 1994, "Mactaquac Generating Station Intake and Spillway Remedial Measures," *ICOLD 18th Congress*, Durban, South Africa, pp. 349-365.

Ulm, F. J.; Coussy, O.; Kefei, L.; and Larive, C., 2000, "Thermo-Chemo-Mechanics of ASR Expansion in Concrete Structures," *Journal of Engineering Mechanics*, Mar., pp. 233-242.

Wagner, C. D., and Newell, V. A., 1995, "A Review of the History of AAR at Three of the TVA's Dam," *Proceedings of the Second International Conference on AAR in Hydroelectric Plants and Dams*, Tenn., Oct., pp. 57-66.

Wittmann, F. H.; Rokugo, K.; Bruhwiler, E.; Mihashi, H.; and Simonin, P., 1988, "Fracture Energy and Strain Softening of Concrete as Determined by Means of Compact Tension Specimens," *Materials and Structures*, V. 21, pp. 21-32.

Zhu, B., 1985, "Prediction of Water Temperature in Reservoirs," *Chinese Journal of Hydraulic Engineering*, No. 2.